OPEN EUROPEAN JOURNAL ON VARIABLE STARS
http://oejv.physics.muni.cz
March 2022 DOI: 10.5817/OEJV2022-0223 ISSN 1801–5964

CCD PHOTOMETRY, PERIOD ANALYSIS AND EVOLUTIONARY STATUS OF THE PULSATING VARIABLE TYC 3292-1328-1

Alton, Kevin B.[1]

1) Desert Blooms Observatories, 70 Summit Ave., Cedar Knolls, NJ 07927, USA,
mail@underoakobservatory.com

Abstract: Multi-color (BVI$_c$) CCD-derived photometric data were acquired from TYC 3292-1328-1, a pulsating variable classified as a high amplitude δ Scuti-type (HADS) system. Analysis of precise time-series lightcurve (LC) data was accomplished using discrete Fourier transformation which revealed a mean fundamental mode (f_0) of oscillation at 10.20831 $\pm$0.00027 d^{-1} along with five other partial harmonics ($2f_0$ and $6f_0$). No other statistically significant frequency shared by all bandpasses was resolved following successive pre-whitening of each residual signal. While no other times-of-maximum were found in the literature, 26 new ToMx values are reported herein. The evolutionary status, age and physical nature of TYC 3292-1328-1 were modeled using the PAdova & TRieste Stellar Evolution Code (PARSEC) for generating stellar tracks and isochrones. At this time, all available results for TYC 3292-1328-1 are consistent with its classification as a HADS variable.

1 Introduction

High amplitude δ Scuti stars, hereafter HADS, constitute a very small percentage (<1%) of all δ Sct variables (Lee et al., 2008). They commonly oscillate (ΔV-mag>0.1) via low-order single or double radial pulsation modes (Poretti , 2003a,b; Niu et al., 2013, 2017) driven by the κ-mechanism resulting from partial ionization of He II (Pamyatnykh , 1999). Many ($\sim$40%) are double pulsators showing simultaneous pulsations in the fundamental and the first overtone mode with amplitudes generally higher in the fundamental mode (McNamara, 2000). Non-radial pulsations have also been detected with the HADS variable V974 Oph (Poretti , 2003a,b). HADS variables have historically been divided according to metallicity relative to the Sun ([Fe/H]=0). The metal-poor ([Fe/H]<<0) group is classified as SX Phe-like stars based on the prototype SX Phoenicis. Ostensibly they have shorter periods (0.02<P<0.125 d) and lower masses ($\sim$1.0-1.3 M$_\odot$) than their related HADS variables possessing near solar metal abundance (McNamara, 2011). SX Phe stars frequently reside in globular clusters (GC) which are ancient collections of Population II stars. Therein, the majority of these pulsators are classified as blue straggler stars, paradoxically appearing much younger than their GC cohorts. Balona & Nemec (2012) proposed that it is not possible to differentiate between δ Sct and field SX Phe variables based on pulsation amplitude, the number of pulsation modes, period or for that matter, even metallicity (Garg et al., 2010). Highly sensitive space telescopes like Kepler (Gilliland et al., 2010), CoRoT (Baglin, 2003) and MOST (Walker et al., 2003) have discovered many examples that contradict these traditionally accepted definitions.

March 2022 DOI: 10.5817/OEJV2022-0223 ISSN 1801–5964

Balona & Nemec (2012) further contend that the evolutionary status of each star is the only way to distinguish between these two classes.

An additional classification scheme for δ Scuti stars was recently proposed by Qian et al. (2017). Therein two distinct groups of δ Scuti stars were uncovered from the LAMOST survey (Zhou et al., 2009) that fundamentally differed in effective temperature. One group was identified as normal δ Scuti stars (NDSTs) when T_{eff} ranged between 6700-8500 K while the other was considered unusual and cool variable stars (UCVs) with T_{eff} values less than 6700 K. A more restrictive fundamental pulsation range (0.09-0.22 d) coupled with being slightly metal poor ([Fe/H]=-0.25-0.0) further differentiates the UCVs from the NDST group. Furthermore, once the UCV stars were excluded from consideration, empirically based temperature-period, log g-period, and metallicity-period relationships were developed for NDSTs.

The variability of TYC 3292-1328-1 (NSVS 3894944, NSVS 1773371 and NSVS 3923574) was first recorded in unfiltered photometric data collected (1999-2000) during the ROTSE-I Survey (Akerlof et al., 2000). These sparsely sampled LC data collected between 1999-2000 were mined from the Northern Sky Variable Survey[1] (Woźniak et al., 2004) for further evaluation. Similarly, photometric (V-mag) data from TYC 3292-1328-1 were also acquired during the All Sky Automated Survey for Supernovae[2] (Shappee et al., 2014) and the SuperWASP Survey [3] (Butters et al., 2010). This report marks the first multi-color photometric study on TYC 3292-1328-1 which also describes the physical nature of this radial pulsator and critically assesses its classification as a HADS variable.

2 Observations and Data Reduction

Time-series images were acquired at Desert Blooms Observatory (DBO, USA - 110.257 W, 31.941 N) with an SBIG STT-1603ME CCD camera mounted at the Cassegrain focus of a 0.4-m ACF-Cassegrain telescope. This telecompressed (0.62×) f/6.8 instrument produced an image scale of 1.36 arcsec/pixel (bin=2×2) and a field-of-view (FOV) of 17.3'× 11.6'. Image acquisition (75-s) was performed using *TheSkyX Pro* Version 10.5.0 (Software Bisque). The CCD-camera is equipped with B, V and I_c filters manufactured to match the Johnson-Cousins Bessell prescription. Dark subtraction, flat correction and registration of all images collected at DBO were performed with *AIP4Win* v2.4.0 (Berry & Burnell , 2005). Instrumental readings were reduced to catalog-based magnitudes using the APASS star fields (Henden et al., 2009, 2010, 2011; Smith et al., 2011) built into *MPO Canopus* v10.7.1.3 (Minor Planet Observer). LCs for TYC 3292-1328-1 were generated using an ensemble of three non-varying comparison stars. The identity, J2000 coordinates and APASS color indices (B-V) for these stars are provided in Table 1. Data from images taken below 30° altitude (airmass >2.0) were excluded. Given that all program stars share the same FOV, differential atmospheric extinction was ignored. During each imaging session comparison stars typically stayed within ±0.009 mag for V and I_c filters and ±0.018 mag for B passband.

[1] https://skydot.lanl.gov/nsvs/nsvs.php
[2] https://asas-sn.osu.edu/variables
[3] https://exoplanetarchive.ipac.caltech.edu

OPEN EUROPEAN JOURNAL ON VARIABLE STARS
http://oejv.physics.muni.cz
March 2022 DOI: 10.5817/OEJV2022-0223 ISSN 1801–5964

Table 1: Astrometric coordinates (J2000), V-mag and color indices (B-V) for TYC 3292-1328-1 and three comparison stars (1-3) used during this photometric study.

FOV ID	Star Identification	R.A. h m s	Dec. deg m s	APASS[a] V-mag	APASS[a] (B-V)
T	TYC 3292-1328-1	01 56 15.5648	+52 26 54.906	11.873	0.448
1	GSC 3292-01845	01 56 03.7266	+52 28 18.086	11.317	0.321
2	GSC 3292-01280	01 57 03.5571	+52 27 16.958	11.200	0.568
3	GSC 3292-01516	01 57 13.5050	+52 24 28.549	10.953	0.143

a: V-mag and (B-V) derived from APASS DR9 database

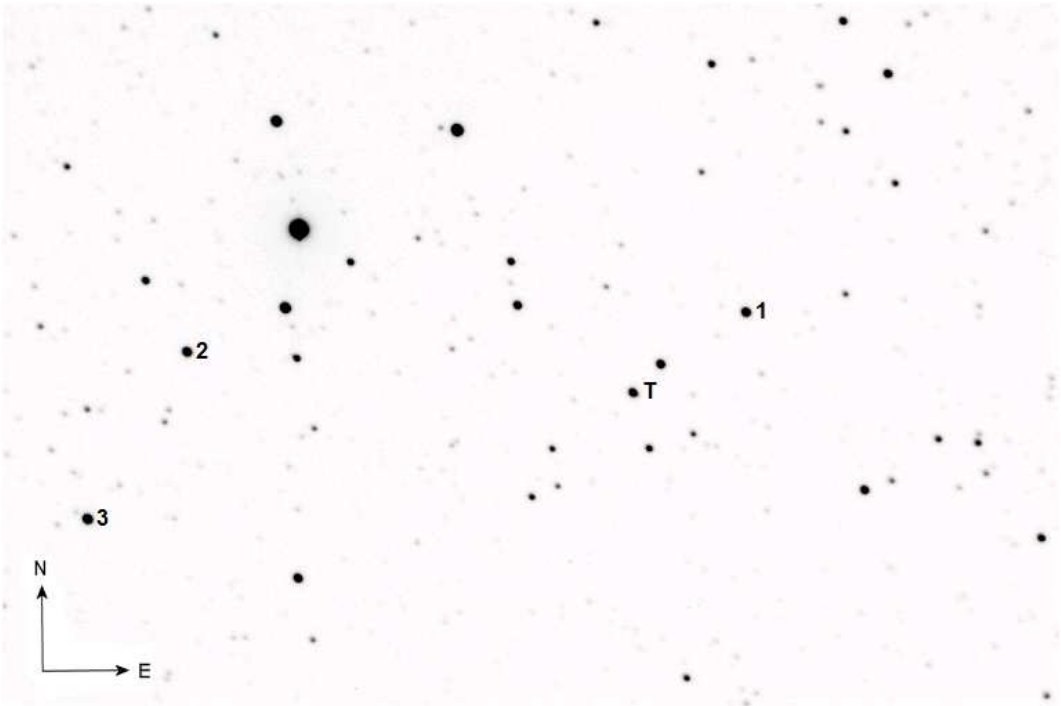

Figure 1: FOV (17.3 × 11.6 arcmin) containing TYC 3292-1328-1 (T) along with the three comparison stars (1-5) used to reduce time-series images to APASS-catalog based magnitudes.

March 2022 DOI: 10.5817/OEJV2022-0223 ISSN 1801–5964

3 Results

Photometric values in B (n=408), V (n=409), and I_c (n=402) passbands were each processed to produce LCs that spanned from 29Dec2017 and 29Nov2018 (Fig. 2). In this case a mean period solution for all passbands (0.0979596 ±0.0000005 d) was obtained using the Fourier curve fitting utility (Harris et al., 1989, FALC) featured in *MPO Canopus* v10.7.1.3. Thereafter, period determinations on survey data (NSVS, ASAS-SN and SuperWASP) were performed using *Peranso v2.6* by applying periodic orthogonals (Schwarzenberg-Czerny, 1996) to fit observations and analysis of variance to assess fit quality. Folding together the sparsely sampled NSVS (1999-2000) survey data revealed a LC period at 0.097960 ±0.000006 d (Fig. 4) while data from the SuperWASP survey (2007) produced a LC (Fig. 5) when P= 0.097959 ±0.000016 d. ASAS-SN (Shappee et al., 2014) photometric data acquired in 2014-2017 were period folded and reached a best fit when P=0.097960 ±0.000003 d (Fig. 6). ToMx estimates (Table 2) were derived using the polynomial extremum fit utility featured in *Peranso v2.6* (Paunzen & Vanmunster, 2016). Since no ToMx data for this variable star were found in the literature only new maxima from DBO (n=10), three interpolated from NSVS and ASAS-SN LCs and 13 others derived from the SuperWASP survey were used to analyze fundamental pulse period timings (PPT). These PPT residuals vs. cycle number (Table 2) can be described by a straight line relationship (Fig. 3) from which a new linear ephemeris was calculated as follows (Eq. 1):

$$Max(HJD) = 2\,458\,451.7206(1) + 0.0979596(1)\ E\,. \tag{1}$$

These results along with the LCs from NSVS, SuperWASP, ASAS-SN and DBO, also suggest that fundamental pulsation period has been largely unchanged since 1999. One curious finding from the survey data that can't be ignored finds that the pulsation amplitude appears to have increased significantly over time. During the ROTSE-I campaign (1999-2000) ΔV-mag from transformed unfiltered photometric data was estimated to be 0.120 mag (Fig. 4) while in 2007 (Fig. 5) ΔV-mag from the SuperWASP survey had increased to 0.223. ASAS-SN LC data (ΔV-mag=0.497) acquired since 2014 (Fig. 6) are nearly superimposable with V-mag data acquired between 2017 and 2018 at DBO. This disparity is unexpected since similar comparisons from HADS variables made by this investigator (Alton , 2019; Alton & Stępień, 2019a,b) have never exhibited such large differences. For a variety of reasons described by Bowman et al. (2016) and Guzik (2021) it is not uncommon to observe amplitude modulation with δ Scuti stars, however, these are normally measured in <100 mmag amounts. Given the long-term duration of the observed changes in amplitude, simple beating between two close frequencies, binarity and a star spot can be safely discounted. The "Blazhko Effect" (Blazhko , 1922), historically attributed to amplitude variability in RR Lyrae-type pulsators, has also been reported for a few HADS variables including V1162 Ori (Arentoft & Sterken, 2002) and GP And (Zhou & Jiang , 2011). However, in neither case did the amplitude vary by any more than 75 mmag. Although there is no direct evidence, one might speculate that dimming could result from the periodic transit of a dusty body associated with a distant orbiting star not unlike that first proposed by Hack (1962) for ϵ Auriga. Should dimming occur again,

March 2022 DOI: 10.5817/OEJV2022-0223 ISSN 1801–5964

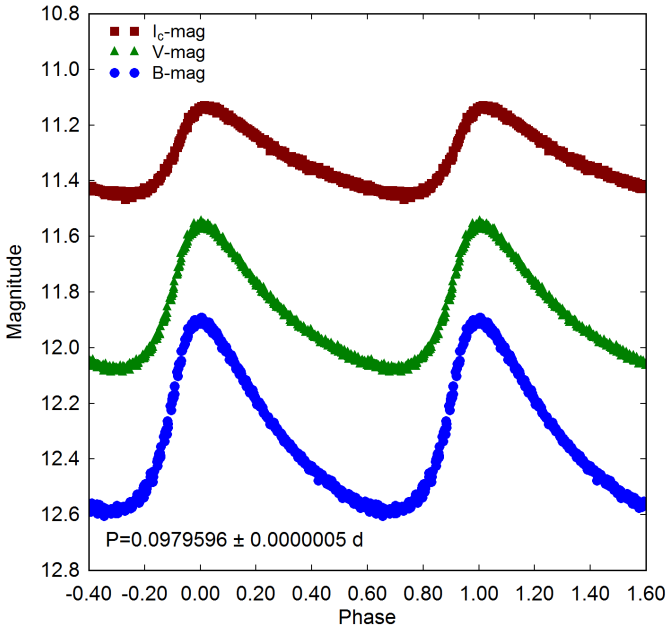

Figure 2: Period folded (0.0979596 ±0.0000005 d) LCs for TYC 3292-1328-1 produced from photometric data obtained between 29Dec2017 and 29Nov2018 at DBO. LCs shown at the top (I_c), middle (V) and bottom (B) represent catalog-based (APASS) magnitudes determined using *MPO Canopus*.

TYC 3292-1328-1 may prove to be an interesting target for spectroscopic and photometric study over the ensuing years.

3.1 Light Curve Behavior

Characteristically, light curves from HADS variables are asymmetrical with rapid brightening to produce a sharply defined maximum peak. Thereafter, slow ascent in magnitude results in a broad minimum. With TYC 3292-1328-1 the largest difference between maximum and minimum light is observed in the blue passband (ΔB-mag = 0.69), followed by V (ΔV-mag = 0.52) and lastly the smallest difference detected in infrared (ΔI_c-mag = 0.32). Plotting (B-V) against phase (Fig. 7) shows significant reddening going from maximum light to minimum light, a behavior commonly observed with pulsating F- to A-type stars.

Interstellar extinction was obtained according to the galactic dust map model revised by Schlafly & Finkbeiner (2011)[4]. The reddening value (E(B-V)=0.2202 ±0.0445 mag) correction corresponds to an intrinsic color index $(B\text{-}V)_0$ for TYC 3292-1328-1 that varies between 0.126 ±0.047 at maximum light and 0.289 ±0.046 mag at minimum brightness. The mean effective temperature (T_{eff}) was estimated by combining results from the polynomial transformation equations derived by Flower (1996), interpolation from Table 5 in Pecaut & Mamajeck (2013) and thirdly, B-V transformations (Warner, 2007) from the 2MASS survey. Not unexpectedly, this mean reddening corrected value (7548 ±354 K) is

[4]https://irsa.ipac.caltech.edu/applications/DUST/

http://oejv.physics.muni.cz
March 2022 DOI: 10.5817/OEJV2022-0223 ISSN 1801–5964

Table 2: Times of maximum (ToMx), measurement uncertainty, filter, epoch and fundamental pulsation timing differences (PTD) for TYC 3292-1328-1 used to calculate a new linear ephemeris.

ToMax (HJD-2400000)	Err	Cycle No.	PTD	Reference
51338.8760	0.0010	-72610	-0.0013	1
51470.6310	0.0010	-71265	-0.0019	1
54339.5747	0.0020	-41978	0.0003	2
54344.5704	0.0014	-41927	0.0001	2
54347.6077	0.0018	-41896	0.0006	2
54348.6847	0.0014	-41885	0.0001	2
54354.5624	0.0018	-41825	0.0002	2
54360.6364	0.0019	-41763	0.0007	2
54362.5948	0.0019	-41743	0.0000	2
54362.6927	0.0017	-41742	-0.0001	2
54363.5758	0.0016	-41733	0.0013	2
54363.6725	0.0017	-41732	0.0001	2
54368.6690	0.0017	-41681	0.0007	2
54381.6972	0.0019	-41548	0.0002	2
54396.5871	0.0018	-41396	0.0002	2
54398.5461	0.0019	-41376	0.0000	2
54402.6618	0.0016	-41334	0.0014	2
54437.4362	0.0018	-40979	0.0003	2
57048.7427	0.0010	-14322	-0.0012	3
58116.6984	0.0004	-3420	-0.0005	4
58117.5801	0.0004	-3411	-0.0004	4
58117.6778	0.0004	-3410	-0.0007	4
58118.6572	0.0004	-3400	-0.0009	4
58131.5882	0.0003	-3268	-0.0006	4
58131.6864	0.0003	-3267	-0.0004	4
58449.6642	0.0006	-21	0.0008	4
58449.7621	0.0009	-20	0.0006	4
58451.6229	0.0005	-1	0.0003	4
58451.7207	0.0006	0	0.0001	4

1. NSVS; 2 SuperWASP; 3; ASAS-SN; 4. This study at DBO

March 2022 DOI: 10.5817/OEJV2022-0223 ISSN 1801–5964

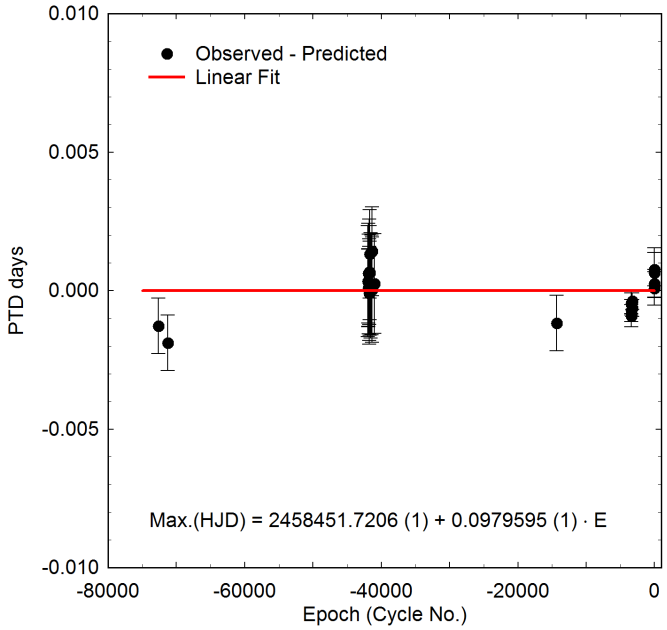

Figure 3: Straight line fit of pulsation timing difference (PTD) vs. period cycle number between 09June1999 and 29Nov2018.

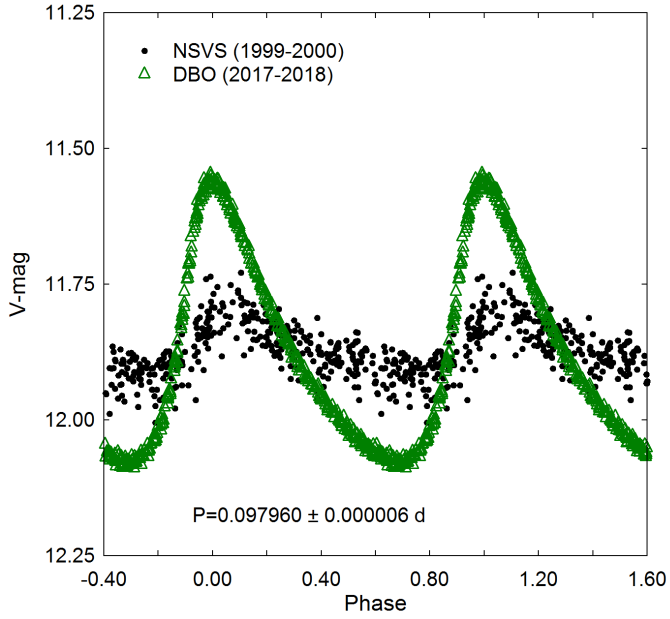

Figure 4: Period folded (0.097960 ±0.000006 d) LCs for TYC 3292-1328-1 produced with sparsely sampled data from the NSVS (1999-2000) Survey. Precise time-series V-mag data acquired at DBO (2017-2018) are superimposed for direct comparison with ROTSE-I magnitudes which have been offset to match the mean DBO-derived value.

March 2022 DOI: 10.5817/OEJV2022-0223 ISSN 1801–5964

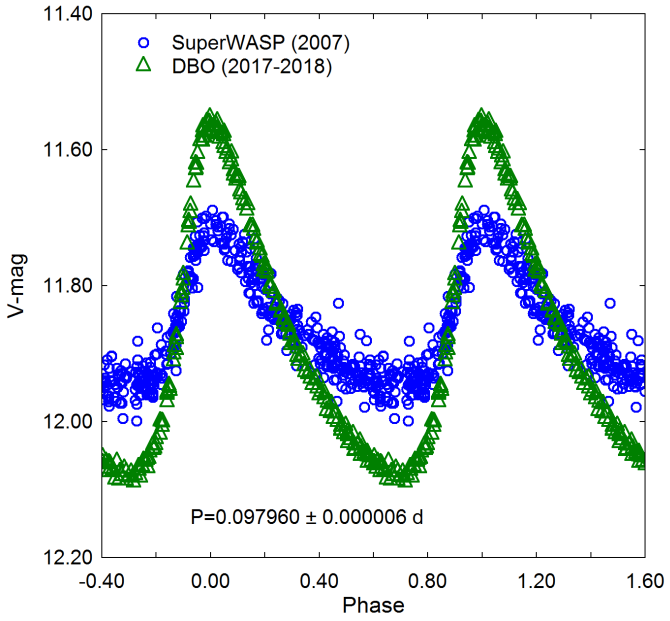

Figure 5: Period folded (0.097960 ±0.000006 d) LCs for TYC 3292-1328-1 produced from CCD-derived photometric data (2007) from the SuperWASP archives. Precise time-series V-mag data acquired at DBO (2017-2018) are superimposed for direct comparison with the SuperWASP data which have been offset to match the mean DBO-derived value.

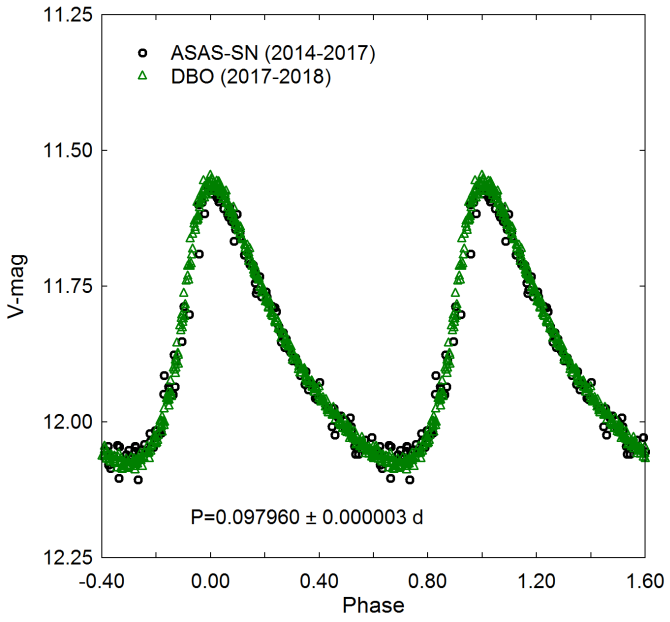

Figure 6: Period folded (0.097960 ±0.000003 d) LCs for TYC 3292-1328-1 produced with photometric data from the ASAS-SN survey (2014-2017). Precise time-series V-mag data acquired at DBO (2017-2018) are superimposed for direct comparison with ASAS-SN magnitudes which have been offset to match the mean DBO-derived value.

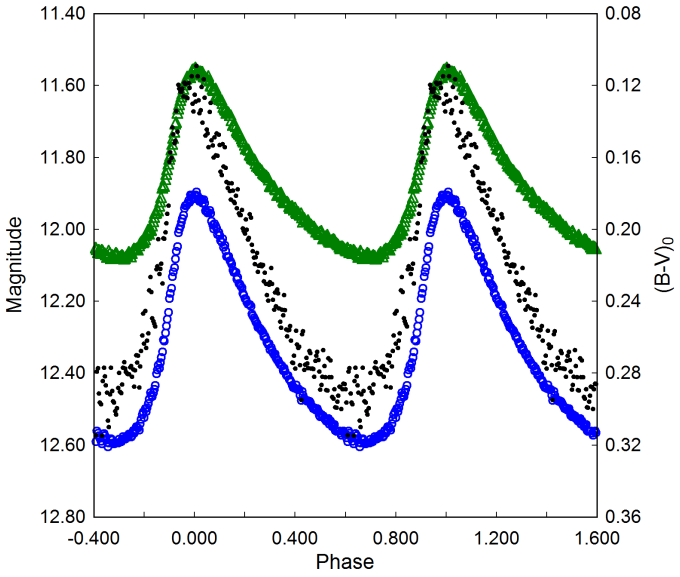

Figure 7: TYC 3292-1328-1 LC illustrating significant increase in reddening as maximum light slowly descends to minimum light (B-V≃0.29 mag). This effect is most closely associated with a decrease in the effective surface temperature (ΔT= 980 K) during minimum light.

higher than the estimate (T_{eff}=6827 $^{+484}_{-218}$ K) in the Gaia DR2 release of stellar parameters which is uncorrected for interstellar extinction (Andrae et al., 2018). The spectral type of this variable would likely range between A7 and A8. According to Qian et al. (2017), TYC 3292-1328-1 would be considered an NDST rather than a UCV since T_{eff} is between 6700 and 8500 K.

3.2 Lightcurve Analysis by Discrete Fourier Transformation

Discrete Fourier transformation (DFT) was used to extract the fundamental pulsating frequency (spectral window = 100 d^{-1}) using *Period04* (Lenz & Breger, 2004). Pre-whitening steps which successively remove the previous most intense signals were employed to reveal other potential oscillations from the residuals. Only those frequencies with a S/N≥6 (Baran et al. , 2014) in each passband are presented in Table 3. In all cases, uncertainties in frequency, amplitude, and phase were estimated by the Monte Carlo simulation (n=400) routine featured in *Period04*. Representative DFT amplitude spectra (f_0–$6f_0$) from V-mag data acquired at DBO are shown in Figure 8. A model fit with residuals based on the elements derived from DFT is shown (Figure 9) for a representative imaging session (30Dec2017). Furthermore, the amplitude decay appears to be exponential as a function of harmonic order (Figure 10), a behavior that has been observed with other HADS variables such as VX Hya (Templeton et al., 2009), V460 And (Alton & Stępień, 2019a) and V524 And (Alton & Stępień, 2019b). LC data acquired from the SuperWASP survey during 2007 were also subjected to DFT decomposition using the same spectral window (*Period*04). The only statistically significant (S/N>6) signals arose from essentially the same fundamental frequency (f_0=10.20857 ±0.00113) and corresponding partial

March 2022 DOI: 10.5817/OEJV2022-0223 ISSN 1801–5964

Table 3: Fundamental frequency (d^{-1}) and corresponding partial harmonics detected following DFT analysis of time-series photometric data (BVI_c) from TYC 3292-1328-1 acquired at DBO

	Freq. (d^{-1})	Freq. Err	Amp. (mag)	Amp. Err	Phase	Phase Err	Amp. S/N
f_0-B	10.20849	0.00010	0.30224	0.00109	0.30361	0.00059	208.96234
f_0-V	10.20822	0.00022	0.22649	0.00182	0.99629	0.00176	232.82545
f_0-I_c	10.20822	0.00012	0.13607	0.00062	0.15293	0.00072	103.40066
$2f_0$-B	20.41668	0.00026	0.10477	0.00110	0.21590	0.00161	147.03125
$2f_0$-V	20.41652	0.00055	0.08134	0.00061	0.92701	0.00476	129.91436
$2f_0$-I_c	20.41645	0.00032	0.05073	0.00061	0.71964	0.00196	55.01564
$3f_0$-B	30.62487	0.00067	0.04219	0.00109	0.84729	0.00421	26.28531
$3f_0$-V	30.62476	0.00185	0.03219	0.00237	0.76618	0.01025	24.78905
$3f_0$-I_c	30.62467	0.00055	0.01930	0.00061	0.29040	0.00516	24.55748
$4f_0$-B	40.83410	0.00150	0.01966	0.00106	0.66391	0.00870	14.49565
$4f_0$-V	40.83410	0.00312	0.01454	0.00198	0.80440	0.02607	13.56923
$4f_0$-I_c	40.83290	0.00177	0.00920	0.00061	0.87837	0.01071	19.33249
$5f_0$-B	51.04015	0.41555	0.01078	0.00146	0.34181	0.13836	10.82560
$5f_0$-V	51.04199	0.05429	0.00806	1.71335	0.41852	0.26095	16.82381
$5f_0$-I_c	51.11420	0.00321	0.00497	0.00249	0.31946	0.01957	10.44025
$6f_0$-V	61.24729	0.01099	0.00511	0.00249	0.32246	0.05955	12.91650

harmonics between $2f_0$ and $6f_0$

3.3 Global Parameters

Well over 100 years ago Henrietta Leavitt discovered a period-luminosity relationship (PLR) from Cepheid variables in the Small Magellanic Cloud (Leavitt & Pickering, 1912) and ever since pulsating stars have endured as standard candles for estimating cosmic distances. This PLR was refined later on to reconcile differences between metal rich (Population I) and metal-poor (Population II) Cepheids (Baade, 1956). Like Cepheids, other variable stars that pulsate via the κ-mechanism were found to obey distinct PLRs. The earliest PLRs for δ Sct variables were published by Frolov (1969) and Dworak & Zieba (1975). An improvement of the PLR for δ Sct variables was reported by McNamara (2011) albeit with Hipparcos parallaxes. A new PLR using, for the most part, more accurate distance values determined by the Gaia Mission (Lindegren et al., 2016; Brown et al., 2018) was recently published (Ziaali et al., 2019). Accordingly this empirically-derived expression (Eq. 2):

$$M_V = (-2.94 \pm 0.06)\ log(P) - (1.34 \pm 0.06)\,, \tag{2}$$

is similar to the equation published by McNamara (2011) but with somewhat less uncertainty.

Absolute V_{mag} (M_V) was estimated (1.58 $\pm$0.09) after substituting the fundamental pulsation period (0.09795956 d) into Eq. 2. The reddening corrected distance modulus

OPEN EUROPEAN JOURNAL ON VARIABLE STARS
http://oejv.physics.muni.cz
March 2022 DOI: 10.5817/OEJV2022-0223 ISSN 1801–5964

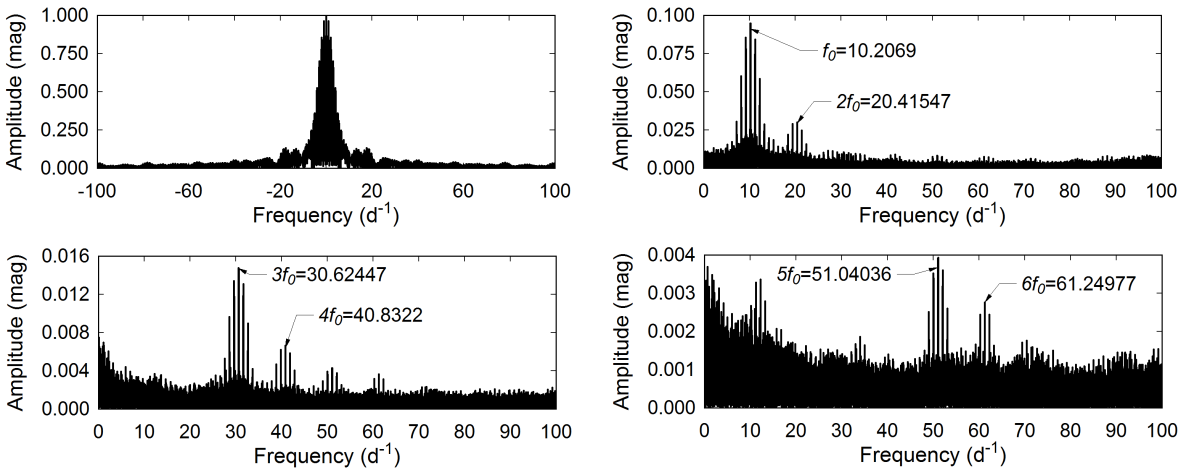

Figure 8: Spectral window (top left) and amplitude spectra showing all significant pulsation frequencies following DFT analysis of V-mag photometric data from TYC 3292-1328-1 acquired at DBO. This includes the fundamental f_0 frequency through its highest partial harmonic $6f_0$ which was detected (S/N≥6) following prewhitening.

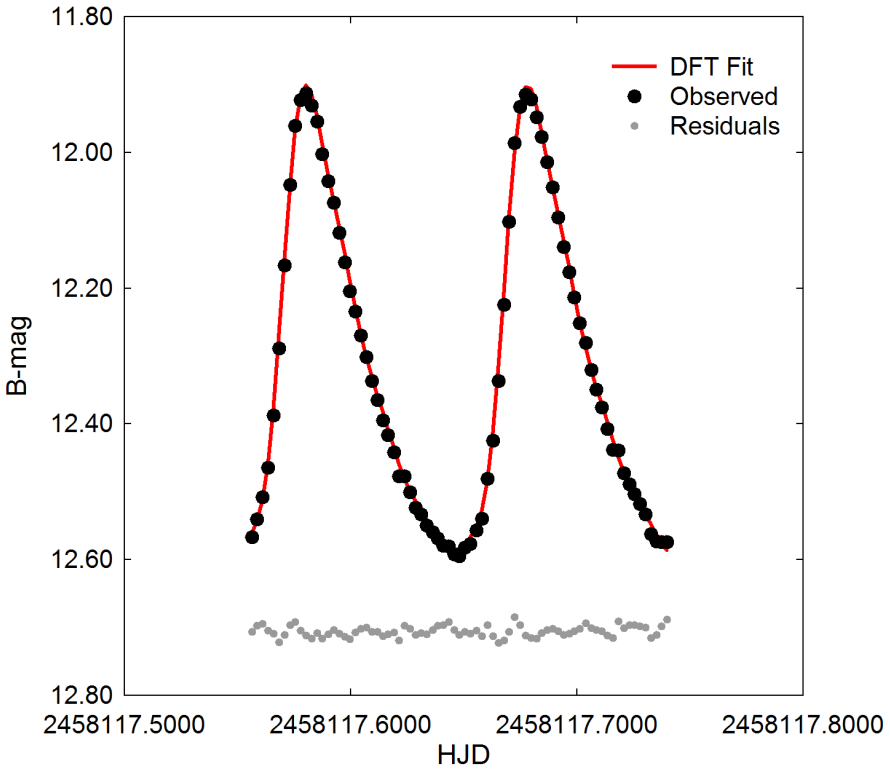

Figure 9: Model fit based on elements derived from DFT for a representative imaging session (30Dec2017) of B-mag LC data. Residuals are offset by a constant amount to compress y-axis scale.

March 2022 DOI: 10.5817/OEJV2022-0223 ISSN 1801–5964

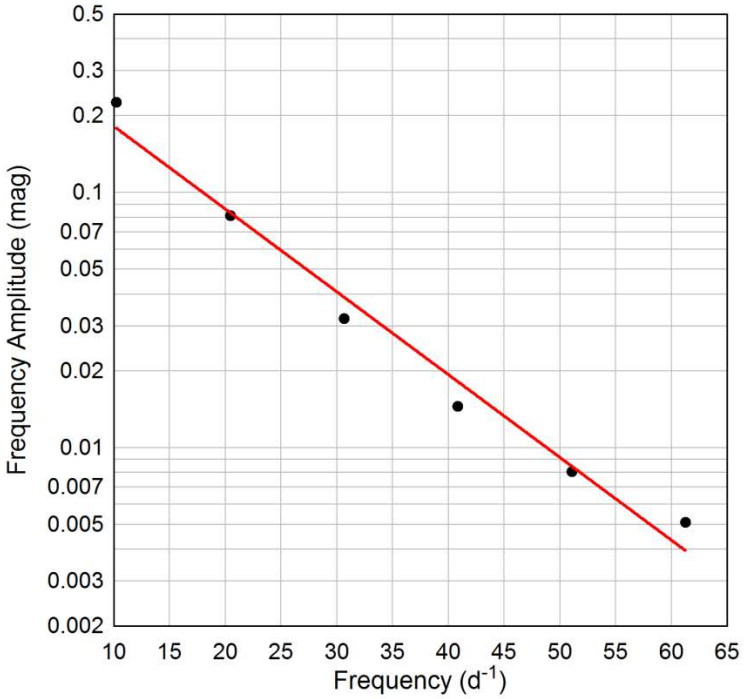

Figure 10: Amplitude decay of the fundamental (f_0) pulsation period and its corresponding partial harmonics ($2f_0$—$6f_0$) observed in the B-passband from LCs acquired at DBO.

(Eq. 3):

$$d(pc) = 10^{(m-M_V-A_V+5)/5)} \tag{3}$$

produced an estimated distance (846 ±35 pc) to TYC 3292-1328-1 from DBO observed values for m (V_{avg}=11.82 ±0.01) and A_V (0.6098 ±0.0214). This result is very similar to the Gaia-DR2 distance (871 $^{+34}_{-31}$ pc) calculated from parallax using the Bailer-Jones bias correction (Bailer-Jones, 2015). TYC 3292-1328-1 is positioned ∼139 pc below the Galactic plane suggesting residence in the thin disc (Li & Zhao, 2017) rather than the old thick disk or halo where many metal poor ([Fe/H]<-1.6) stars like SX Phe-type variables reside (Carollo et al., 2010).

Gaia DR2 also includes estimates for radius and luminosity (Andrae et al., 2018). In this regard it is worth examining some differences in the equations used to produce the Gaia DR2 values reported for TYC 3292-1328-1 and those otherwise determined herein. This has been discussed in more detail for two other HADS variables V460 And (Alton & Stępień, 2019a) and V524 And (Alton & Stępień, 2019b). The Gaia passbands (BP, G and RP) are unique (Jordi et al. 2010) so that transforms are needed. Since color excess (B-V) has been determined in this study, Gaia G-magnitudes can be transformed to Johnson-Cousins V_{mag} according to the following expression (Eq. 4):

$$G - V = a + b(B-V) + c(B-V)^2 + d(B-V)^3\,, \tag{4}$$

in which a-d are the Johnson-Cousins coefficients[5]. V_{mag} was subsequently calculated to

[5]https://gea.esac.esa.int/archive/documentation/GDR2/Data_processing/chap_cu5pho/sec_cu5pho_calibr/

be 11.93 ±0.03, a result that is reasonably close to V_{avg} (11.82 ±0.01) observed in this study. Derivation of stellar parameters first released from the Gaia Mission is described in detail by Andrae et al. (2018). Absolute G-band magnitude (M_G) is estimated according to Eq. 5:

$$M_G = G - 5 \cdot log_{10}(r) + 5 - A_G\,, \tag{5}$$

where G is the photometric system magnitude, r=1/π (π = parallax in arcsec) and A_G is the interstellar extinction. The assumed null value for A_G is an important distinction since non-Gaia data such as those determined from independently derived galactic dust map models are not used to produce absolute magnitude estimates.

Notably, TYC 3292-1328-1 resides in a dusty region of the Milky Way (Gal. coord. (J2000): l = 132.8532; b = -9.1701 where interstellar extinction (A_V=0.6098 ±0.0214) is measurably different from zero (Schlafly & Finkbeiner, 2011). Extinction corrected luminosity in solar units was calculated according to Eq. 6:

$$\frac{L_*}{L_\odot} = 10^{((M_{bol\odot} - M_{bol*})/2.5)}\,, \tag{6}$$

where $M_{bol\odot}$ = 4.74, M_V=1.511 ±0.084 and BC_V=0.0331. The result (L_*=18.99 ±1.47 $L_\odot$) is significantly greater than the uncorrected Gaia DR2 estimate (10.21 $^{+0.57}_{-0.57}$ $L_\odot$) which assumes A_G=0. Finally, the radius in solar units (R_*= 2.55 ±0.26) was estimated using the well-known relationship (Eq. 7) where:

$$\frac{L_*}{L_\odot} = \Big(\frac{R_*}{R_\odot}\Big)^2 \Big(\frac{T_*}{T_\odot}\Big)^4\,. \tag{7}$$

It follows that the final result calculated for $R_\odot$ using Eqs. 6 and 7 is higher than that reported for $R_\odot$ ($2.28^{+0.16}_{-0.29}$) in Gaia DR2.

Pulsation period, luminosity and temperature/color can be measured by observation, however, the mass of a single isolated field star like TYC 3292-1328-1 is very difficult to determine directly. According to Eker et al. (2018), under certain conditions ($1.05<M_\odot\leq 2.40$) it is possible to estimate the mass of a lone star according to a mass-luminosity relationship derived from main sequence (MS) stars in detached binary systems. This expression (Eq. 8):

$$log(L) = 4.329(\pm 0.087) \cdot log(M) - 0.010(\pm 0.019), \tag{8}$$

leads to a mass (1.98 ±0.04 $M_\odot$) derived when $L_\odot$=18.99 ±1.47. Fairly typical for a HADS variable, this result along with derived values for density ($\rho_\odot$), surface gravity (log g), and pulsation constant (Q) are also included in Table 4.

Stellar density (ρ_*) in solar units (g/cm^3) was calculated according to Eq. 9:

$$\rho_* = 3 \cdot G \cdot M_* \cdot m_\odot / (4\pi (R_* \cdot r_\odot)^3)\,, \tag{9}$$

where G is the cgs gravitational constant, $m_\odot$=solar mass (g), $r_\odot$=solar radius (cm), M_* is the mass and R_* the radius of TYC 3292-1328-1 in solar units. Using the same algebraic assignments, surface gravity (log g) was determined by the following expression (Eq. 10):

$$log\ g = log(M_* \cdot m_\odot / (R_* \cdot r_\odot)^2)\,. \tag{10}$$

ssec_cu5pho_PhotTransf.html#Ch5.T8

March 2022 DOI: 10.5817/OEJV2022-0223 ISSN 1801–5964

Table 4: Global stellar parameters for TYC 3292-1328-1 using those determined directly from observations at DBO and from PARSEC evolutionary modeling

Parameter	DBO	PARSEC
Mean T_{eff} [K]	7548 ±354	7548 ±354
Luminosity [$L_{\odot}$]	18.99 ±1.47	18.99 ±1.47
Mass [$M_{\odot}$]	1.98 ±0.04	1.91±0.03
Radius [$R_{\odot}$]	2.55 ±0.26	2.60±0.05
ρ [g/cm^3]	0.17 ±0.05	0.15±0.01
log g [cgs]	3.923 ±0.042	3.889±0.018
Q [d]	0.034 ±0.004	0.032±0.004

The dynamical time that it takes a p-mode acoustic wave to internally traverse a star is strongly correlated to the stellar mean density. The pulsation constant (Q) is defined by the period-density relationship (Eq. 11):

$$Q = P\sqrt{\frac{\overline{\rho}_*}{\overline{\rho}_{\odot}}}\,, \tag{11}$$

where P is the pulsation period (d) and $\overline{\rho}_*$ and $\overline{\rho}_{\odot}$ are the mean densities of the target star and Sun, respectively. The mean density can be expressed (Eq. 12) in terms of other measurable stellar parameters where:

$$log(Q) = -6.545 + log(P) + 0.5log(g) + 0.1M_{bol} + log(T_{eff})\,. \tag{12}$$

The full derivation of this expression can be found in Breger (1990). The resulting Q values (Table 4) are similar to what would be expected (Q=0.03-0.04 d) from fundamental radial pulsations observed with other δ Sct variables (Breger & Bregman , 1975; Breger, 1979; Joshi & Joshi et al., 2015; Antonello & Pastori, 2005).

3.4 Evolutionary status of TYC 3292-1328-1

The evolutionary status of TYC 3292-1328-1 was evaluated (Fig. 11) using PARSEC-derived stellar tracks and isochrones (Bressan et al., 2012) and then plotted (log T_{eff} vs. log($L/L_{\odot}$) in a theoretical Hertzsprung-Russell diagram (HRD). The thick solid maroon-colored line defines the zero-age main sequence (ZAMS) position for stars with metallicity Z=0.020. The two broken lines nearly perpendicular to the ZAMS delimit the blue (left) and red (right) edges of the theoretical instability strip for radial low-p modes (Xiong et al. , 2016). Also included are the positions of several known HADS and SX Phe-type variables (Balona , 2018). The solid black circle indicates the position of TYC 3292-1328-1 using the DBO derived parameters (T_{eff} and $L_{\odot}$) provided in Table 4. Interestingly a single undisputed value for the metallicity of our nearest star remains elusive. Over the last few decades, the reference metallicity values used by several authors for computing stellar models have ranged between 0.012 and 0.020 (Amard et al., 2019). Furthermore, Serenelli et al. (2016) was not convinced that a $Z_{\odot}$-value (0.0196 ±0.0014) based on solar wind composition (von Steiger & Zurbuchen, 2016; Vagnozzi , 2017) could be used as a

March 2022 DOI: 10.5817/OEJV2022-0223 ISSN 1801–5964

surrogate to replace traditional spectroscopic estimates of metallicity in the solar interior. A definitive value for $Z_{\odot}$ remains to be determined. Nonetheless, a metal abundance (Z) value is still required in order to predict mass, radius and age of TYC 3292-1328-1 from theoretical evolutionary tracks. A Z-value can be estimated indirectly from its Galactic coordinates in that its distance from the galactic plane (-139 pc) favors a thin disc membership rather than residence in the halo where metal poor stars ([Fe/H]<-1.6) are found. Furthermore, Qian et al. (2017) reports an empirical relationship between metallicity ([Fe/H]) and the fundamental pulsation period P for an NDST star according to the following (Eq. 13)

$$[Fe/H] = -0.121(\pm 0.026) + 0.92(\pm 0.25) \times P\,. \tag{13}$$

The predicted value ([Fe/H]=-0.031 ±0.036) suggests that TYC 3292-1328-1 approaches solar metallicity, or at most a few times lower.

Two separate PARSEC evolutionary models (Bressan et al., 2012) ranging in age between $1{\times}10^8$ and $2.41{\times}10^9$ y are illustrated in Fig. 10. The red lines show the models ($M_{\odot}$=1.875, 1.90 and 1.925) when Z=0.020 while the blue lines define the models ($M_{\odot}$=1.50, 1.55 and 1.60) where Z=0.004. The latter simulations correspond to a decrease in metallicity by a factor of 3 to 5 depending on the reference solar metallicity. Assuming Z=0.020, it can be shown that TYC 3292-1328-1 would have a mass of 1.91 ± 0.03 $M_{\odot}$ and a radius of 2.60 ±0.05 $R_{\odot}$. The position of this intrinsic variable along the $M_{\odot}$=1.90 evolutionary track extrapolates to an age of 1.05 ±0.02 Gyr suggesting it is a moderately evolved MS object lying amongst other HADs closer to the blue edge (left side) of the instability strip.

By comparison, if TYC 3292-1328-1 is a metal poor (Z=0.004) star, then it would have a similar radius (2.53 ± 0.01 $R_{\odot}$), but would be far less massive (1.51 ±0.05 $M_{\odot}$). Its position along the 1.5 $M_{\odot}$ track lies within the HRD region where evolutionary tracks of low metallicity stars begin to zigzag due to a stellar contraction near the end of hydrogen burning in the core. This star would still be a MS object but with an age approaching 1.94 Gyr. The theoretical mass (1.91 $M_{\odot}$) where Z=0.020 favors near solar metallicity of TYC 3292-1328-1. This is also in good agreement with results independently determined (Table 4) using an empirical mass-luminosity relationship. Uncertainty about the mass and metallicity of TYC 3292-1328-1 will likely improve should high resolution spectroscopic data become available in the future.

4 Conclusions

This first multi-color (BVI_c) CCD study of TYC 3292-1328-1 along with survey data from three sources has produced 26 new times-of-maximum. Even with this limited number of values, there does not appear to any secular changes in the fundamental mode of oscillation over the past 20 y. Deconvolution of time-series photometric data by discrete Fourier transformation shows that TYC 3292-1328-1 is a monoperiodic radial pulsator (f_0=10.20831 d^{-1}) which also oscillates in at least 5 other partial harmonics ($2f_0$ through $6f_0$). It is conceivable that a more expansive dataset collected at multiple sites over a much

OPEN EUROPEAN JOURNAL ON VARIABLE STARS
http://oejv.physics.muni.cz
March 2022 DOI: 10.5817/OEJV2022-0223 ISSN 1801–5964

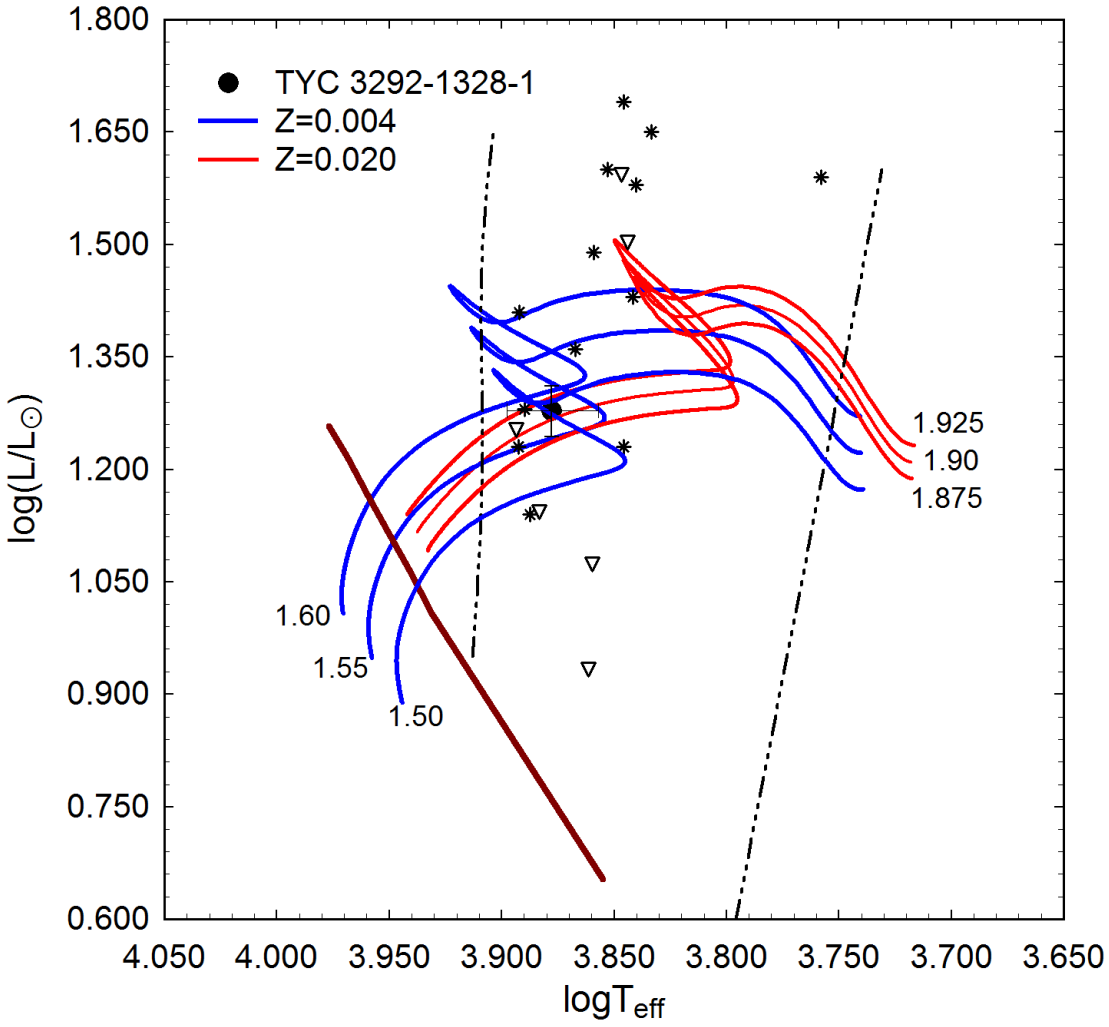

Figure 11: Evolutionary tracks (red lines; Z=0.020 and blue lines; Z=0.004) derived from PARSEC models (Bressan et al. 2012) showing position of TYC 3292-1328-1 (black filled circle) relative to ZAMS (thick maroon line) and within the theoretical instability strip (black dashed lines) for low-order radial mode δ Scuti pulsators. The position of other HADS (*) and SX Phe (open triangle) variables reported by Balona (2018) are included for comparison.

March 2022 DOI: 10.5817/OEJV2022-0223 ISSN 1801–5964

longer period of time could reveal other oscillation modes that were not detected in this study. A mean effective temperature for TYC 3292-1328-1 (7548 ±354 K) was estimated from multiple sources and likely corresponds to spectral type A7-A8. A comparison of results (Table 4) derived from evolutionary modeling and those determined from observations at DBO revealed only minor differences. The pulsation period (∼0.0979959 d), radial oscillation mode, V_{mag} amplitude (0.52 mag), spectral type and LC morphology are all consistent with the defining characteristics of a HADS variable. The generally accepted threshold for SX Phe stars is <1.3 $M_{\odot}$ (McNamara 2011) which in this case is far less than the mass predicted from a M-L relationship (∼1.94-2.02 $M_{\odot}$) and evolutionary modeling (∼1.91 $M_{\odot}$). Given these results, the weight of evidence confirms that TYC 3292-1328-1 is a HADS variable with near solar metallicity.

Acknowledgements: This research has made use of the SIMBAD database operated at Centre de Données astronomiques de Strasbourg, France. The Northern Sky Variability Survey hosted by the Los Alamos National Laboratory, the All Sky Automated Survey for Supernovae and the SuperWASP survey were mined for essential information. This work also presents results from the European Space Agency (ESA) space mission Gaia. Gaia data are being processed by the Gaia Data Processing and Analysis Consortium (DPAC). Funding for the DPAC is provided by national institutions, in particular the institutions participating in the Gaia MultiLateral Agreement (MLA). The Gaia mission website is https://www.cosmos.esa.int/gaia. The Gaia archive website is https://archives.esac.esa.int/gaia. This research was made possible through the use of the AAVSO Photometric All-Sky Survey (APASS), funded by the Robert Martin Ayers Sciences Fund and NSF AST-1412587. The diligence and dedication shown by all associated with these organizations is very much appreciated.

References

Akerlof, C., Amrose, S., Balsano, R., Bloch, J., et al. 2000, *PASP*, **122**, 131, doi:10.1086/301321

Alton, K.B. 2019, *JAAVSO*, **47**, 231, https://www.aavso.org/apps/jaavso/article/3521/

Alton, K.B. & Stępień, K. 2019a, *JAAVSO*, **47**, 53, https://www.aavso.org/apps/jaavso/article/3466/

Alton, K.B. & Stępień, K. 2019b, *Acta Astron.*, **69**, 283, doi:10.32023/0001-5237/69.3.4

Amard, E.B., Palacios, A., Charbonnel, C., Gallet, F., et al. 2019, *arXiv e-prints*, , , https://ui.adsabs.harvard.edu/abs/2019arXiv190508516A

Andrae, R., Fouesneau, M., Creevey, O, Ordenovic, C., et al. 2018, *Astronomy & Astrophysics*, **616**, A8, doi:10.1051/0004-6361/201732516

Antonello, E. & Pastori, L. 1981, *PASP*, **93**, 237, doi:10.1086/130812

Arentoft, T. & Sterken, C, 2002, *Observational Aspects of Pulsating B- and A Stars, ASP Conference Proceedings*, **Vol. 256. Edited by Christiaan Sterken and Donald W. Kurtz.. San Francisco: Astronomical Society of the Pacific, 2002**, 79, 2002ASPC..256...79A

Baade, W. 1956 *PASP*, **68**, 5, doi:10.1086/126870

Baglin, A. 2003 *Advances in Space Research*, **31**, 345, https://www.sciencedirect.com/science/article/pii/S0273117702006245

Bailer-Jones, C.A.L. 2015 *PASP*, **127**, 994, doi:10.1086/683116

Balona, L.A., Nemec, J.M. 2012, *MNRAS*, **426**, 2413, doi:10.1111/j.1365-2966.2012.21957.x

Balona, L.A. 2018, *MNRAS*, **479**, 183, doi:10.1093/mnras/sty1511

Baran, A.S., Koen, C. and Porkrzywka, B. 2014, *MNRAS*, **448**, L16, 10.1093/mnrasl/slu194

Berry, R. and Burnell, J. 2005, *The Handbook of Astronomical Image Processing*, Wilmann-Bell, Inc., Richmond, VA, https://ui.adsabs.harvard.edu/abs/2000haip.book.....B/abstract

Blazhko, S.N. 1922, *Astron. Nach.***216**, 103, doi:10.1002/asna.19222160703

Bowman, D.M., Kurtz, D.W., Breger, M., et al. 2016, *Mon. Not. R. Astron. Soc.*, **460**, 1970, 10.1093/mnras/stw1153

Breger, M. 1979, *PASP*, **91**, 5, doi:10.1086/130433

Breger, M. 1990, *Delta Scuti Star Newsletter*, **1**, 13, http://articles.adsabs.harvard.edu/pdf/1990ASPC...11..263B

Breger, M. and Bregman, J.N. 1975, *Astrophys. J.*, **200**, 343, doi:10.1086/153794

Bressan, A., Marigo, P., Giradi, L., G., Salasnich, B., et al. 2010, *MNRAS*, **427**, 127, doi:10.1111/j.1365-2966.2012.21948.x

Brown, A.G.A., Vallenari, A., Prusti, T., de Bruijne, J.H.J, et al. 2018, *A&A*, **616**, A1, doi:10.1051/0004-6361/201833051

Butters, O.W., West, R.G., Anderson, D.R., Collier Cameron, A., et al. 2010, *A&A*, **520**, L10, doi:10.1051/0004-6361/201015655

Carollo, D., Beers, T.C., Chiba, M., Norris, J.E., et al. 2010 *The Astrophysical Journal*, **712**, 692, doi:10.1088/0004-637x/712/1/692

Dworak, T.Z. & Zieba, S. 1975, *Information Bulletin on Variable Stars*, **1005**, , http://articles.adsabs.harvard.edu/pdf/1975IBVS.1005....1D

Eker, Z., Bakış, V., Bilir, S. et al. 2018, *MNRAS*, **479**, 5491, doi:10.1093/mnras/sty1834

Flower, P.J. 1996, *The Astrophysical Journal*, **469**, 355, doi:10.1086/177785

Frolov, M.S. 1969, *Astronomicheskii Tsirkulyar*, **505**, 1, https://ui.adsabs.harvard.edu/abs/1969ATsir.505....1F/abstract

Garg, A., Cook, K.H., Nikolaev, S., Huber, M.E., et al. 2010, *AJ*, **140**, 328, doi:10.1088/0004-6256/140/2/328

Gilliland, R.L., Brown, T.M., Christensen-Dalsgaard, J., Kjeldsen, H , et al. 2010, *PASP*, **122**, 131, doi:10.1086/650399

Guzik, J.A. 2021, *Frontiers in Astronomy and Space Sciences*, **8**, 55, doi:10.3389/fspas.2021.653558

Hack, M. 1962, *Memorie della Società Astronomia Italiana*, **32**, 351, 1962MmSAI..32..351H

Harris, A.W., Young, J.W., Bowell, E. et al. 1989, *Icarus*, **77**, 171, https://www.sciencedirect.com/science/article/abs/pii/0019103589900158?via%3Dihub

Henden, A.A., Welch, D.L., Terrell, D. and Levine, S.E. 2009 *American Astronomical Society Meeting Abstracts*, **214**, 669, https://ui.adsabs.harvard.edu/abs/2009AAS...21440702H/abstract

Henden, A.A., Terrell, D., Welch, D.L., and Smith, T.C. 2010 *American Astronomical Society Meeting Abstracts*, **215**, 515, https://ui.adsabs.harvard.edu/abs/2010AAS...21547011H/abstract

Henden, A.A., Levine, S.E., Terrell, D., et al. 2011 *American Astronomical Society Meeting Abstracts*, **218**, 126.01, https://ui.adsabs.harvard.edu/abs/2011AAS...21812601H/abstract

Joshi, S. & Joshi, Y.C. 2015, *Journal of Astrophysics and Astronomy*, **36**, 33, doi:10.1007/s12036-015-9327-z

Leavitt, H.S. & Pickering, E.C. 1912, *Harvard College Observatory Circular*, http://articles.adsabs.harvard.edu/full/1912HarCi.173....1L

Lee, Y.-H, Kim, S.S., Shin, J., et al. 2008, *PASJ*, **60**, 3, https://academic.oup.com/pasj/article/60/3/551/1508512

Lenz, P. & Breger, M. 2004, *Proceedings of the International Astronomical Union*, doi:10.1017/s1743921305009750

Li, C. & Zhao, G. 2017, *The Astrophysical Journal*, doi:10.3847/1538-4357/aa93f4

Lindegren, L, Lammers U, Bastian, U., Hernández, J., et al. 2016, *A&A*, **595**, A4, 10.1051/0004-6361/201628714

McNamara, D.H. 2000, *Astronomical Society of the Pacific Conference Series*, **210**, 373, http://articles.adsabs.harvard.edu/pdf/2000ASPC..210..373M

McNamara, D.H. 2011, *AJ*, **142**, 110, doi:10.1088/0004-6256/142/4/110

Niu, J.-S, Fu, J.-N. & Zong, W.-K. 2013, *Research in Astronomy and Astrophysics*, **13**, 1181, doi:10.1088/1674-4527/13/10/004

Niu, J.-S, Fu, J.-N., Li, Y., et al. 2017, *MNRAS*, **467**, 3122, https://academic.oup.com/mnras/article-abstract/467/3/3122/2929269

Pamyatnykh, A.A. 1999, *Acta Astron.*, **49**, 119, http://articles.adsabs.harvard.edu/pdf/1999AcA....49..119P

Paunzen, E. & Vanmunster, T. 2016, *Astronomische Nachrichten*, **337**, 239, doi:10.1002/asna.201512254

Pecaut, M.J. & Mamajek, E.E. 2013, *Astrophys. J. Supplement*, **208**, , doi:10.1088/0067-0049/208/1/9

Poretti, E. 2003a, *A&A*, **409**, 1031, https://www.aanda.org/articles/aa/abs/2003/39/aa3932/aa3932.html

Poretti, E. 2003b, *ASP Conf. Ser. 292*, http://articles.adsabs.harvard.edu/pdf/2003ASPC..292..145P

Qian, S.-B., Li, L.-J., He, J.-J., et al. 2017, *MNRAS*, **475** 478, doi:10.1093/mnras/stx3185

Schwarzenberg-Czerny, A.. 1996, *The Astrophysical Journal*, **460**, L107, doi:10.1086/309985

Schlafly, E.F. & Finkbeiner, D.P. 2011, *The Astrophysical Journal*, **737**, 103, doi:10.1088/0004-637x/737/2/103

Serenelli, A., Scott, P., Villante, F.L., Vincent, A.C., et al. 2016, *MNRAS*, **463**, 2, doi:10.1093/mnras/stw1927

Shappee, B., Prieto, J., Stanek, K.Z, Kochanek, C.S., et al. 2014, *AJ*, **788**, 48, https://aas.org/sites/default/files/2020-01/AAS_223_Abstracts.pdf

Smith, T.C., Henden, A.A., Starkey, D.R. 2011 *Society for Astronomical Sciences Annual Symposium*, **30**, 121, http://articles.adsabs.harvard.edu/pdf/2011SASS...30..121S

Templeton, M.R., Samolyk, G., Dvorak, S., Poklar, R., Butterworth, N., and Gerner, H. 2009 *Pub. Astron. Soc. Pacific*, **121**, 1076, doi:10.1086/630211

Vagnozzi, S., Freese, K & Zurbuchen, T.H. 2017, *Astrophys. J.*, **839**, 55 doi:10.3847/1538-4357/aa6931

von Steiger, R. & Zurbuchen, T.H. 2016, *The Astrophysical Journal*, **816**, 13, doi:10.3847/0004-637x/816/1/13

Walker, G., Matthews, J., Kuschnig, R., et al. 2003, *PASJ*, **115**, 1023, doi:10.1086/377358

March 2022 DOI: 10.5817/OEJV2022-0223 ISSN 1801–5964

Warner, B.D. 2007, *Minor Planet Bulletin*, http://adsabs.harvard.edu/abs/2007MPBu...34..113W

Woźniak, P.R., Vestrand, W.T., Akerlof, C.W., Balsano, R., et al. 2004, *AJ*, **127**, 2436, doi:10.1086/382719

Xiong, D.R., Deng, L., Zhang, C. & Wang, K. 2016, *MNRAS*, **457**, 3163, doi:10.1093/mnras/stw047

Zhou, A.-Y. & Jiang, S.-Y, 2011, *A.J*, **142**, 100, doi:10.1088/0004-6256/142/4/100

Zhou, A.-Y., Jiang, X.-J., Zhang, Y.P. & Wei, J.-Y. 2009, *Research in Astronomy and Astrophysics*, **9**, 349, doi:10.1088/1674-4527/9/3/010

Ziaali, E., Bedding, T.R., Murphy, S.J., et al. 2019, *MNRAS*, **486**, 4348, doi:10.1093/mnras/stz1110